Decoupling interface effect on the phase stability of CdS thin films by van der Waals heteroepitaxy

Xin Sun, Yiping Wang, Lucas J. Seewald, Zhizhong Chen, Jian Shi, Morris A. Washington, and Toh-Ming Lu

Citation: Appl. Phys. Lett. **110**, 041602 (2017); doi: 10.1063/1.4974855

View online: http://dx.doi.org/10.1063/1.4974855

View Table of Contents: http://aip.scitation.org/toc/apl/110/4

Published by the American Institute of Physics

Articles you may be interested in

Insights into the spontaneous formation of silicene sheet on diboride thin films Applied Physics Letters **110**, 041601 (2017); 10.1063/1.4974467

Polarization multiplexing in large-mode-area waveguides and its application to signal enhancement in multiphoton microscopy

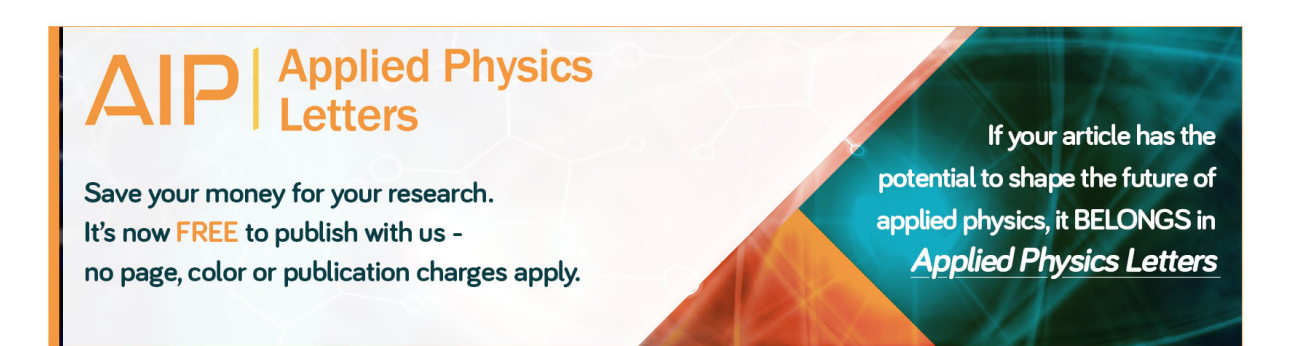
Applied Physics Letters 110, 041101 (2017); 10.1063/1.4974856

Ion capturing/ion releasing films and nanoparticles in liquid crystal devices Applied Physics Letters **110**, 041103 (2017); 10.1063/1.4974453

Optically thin hybrid cavity for terahertz photo-conductive detectors Applied Physics Letters **110**, 041105 (2017); 10.1063/1.4974482

van der Waals epitaxy of CdS thin films on single-crystalline graphene Applied Physics Letters **110**, 153104 (2017); 10.1063/1.4980088

Anisotropic crystallization in solution processed chalcogenide thin film by linearly polarized laser Applied Physics Letters **110**, 041904 (2017); 10.1063/1.4975067





Decoupling interface effect on the phase stability of CdS thin films by van der Waals heteroepitaxy

Xin Sun,^{1,a)} Yiping Wang,² Lucas J. Seewald,¹ Zhizhong Chen,² Jian Shi,² Morris A. Washington,¹ and Toh-Ming Lu¹

¹Department of Physics, Applied Physics and Astronomy, and Center for Materials, Devices and Integrated Systems, Rensselaer Polytechnic Institute, Troy, New York, 12180, USA

(Received 4 November 2016; accepted 12 January 2017; published online 24 January 2017)

Wurtzite (W) and zinc-blende (ZB) polytypism has long been observed in epitaxial CdS thin films. The present work, based on van der Waals epitaxial CdS thin films, is an attempt to explain which crystal modification, W or ZB, is favored under different growth conditions. In this van der Waals epitaxy system where the substrate influence is considered weak, it is found that the substrate temperature plays a crucial role in determining the crystal modification of CdS, that is, W and ZB CdS are more stable at low and high ends of substrate temperature, respectively. We attribute this temperature effect to the entropy difference $(S_W < S_{ZB})$, a conclusion well supported by the thermodynamic hard sphere model formulation of the entropy difference between hexagonal close-packed and face-centered cubic structures. By summarizing other works, we find that the entropy difference model can also be applied to large mismatched (≥3%) CdS-substrate chemical epitaxy systems but not for small mismatched ($\lesssim 3\%$) ones. In the latter case, the energy benefit in terms of high density of bonding contributed by the substrate-film interface is believed to be too overwhelming for the intrinsic entropy difference to overcome. Furthermore, the deposition rate is found to affect the crystalline quality and strain level in CdS films but not the crystal modification of the CdS films. Last, Raman and photoluminescence spectroscopies reveal the strain behaviors in the films. The phase change from W to ZB CdS is well-correlated with the observed peak shifts in Raman and photoluminescence spectroscopies. Published by AIP Publishing. [http://dx.doi.org/10.1063/1.4974855]

CdS is a popular semiconductor with several important applications, including photovoltaics, light emitting diode (LED),² photodetector,³ lasing,⁴ and anti-Stokes cooling.⁵ CdS crystallizes in three forms, namely, wurtzite (W), zincblende (ZB), and rock-salt (RS). RS only exists under highpressure and high-temperature, leaving an understanding of W-ZB polytypism to be more significant in semiconductor research. Unlike many other binary octet compounds, whose structural energies between W and ZB phases are distantly separated, W and the so-called metastable ZB CdS are almost degenerate in energy. This has been frequently verified because CdS is obtained in W modification as often as in ZB. 8-12 The present work concerns only vapor-deposited epitaxial CdS thin films, which have been reported in W, ZB, and W-ZB mixed forms. 13-23 In those studies, the substrate temperature and the substrate crystal structure were speculated to be the main factors in determining the crystal modification of films. Despite having been investigated for decades, the specific role of each factor is still debatable due to conflicting results in the literature.

Herein, we study the crystal modification of epitaxial CdS thin films by separating the effect of substrate temperature from that of the substrate crystal structure or interface effect. van der Waals epitaxy (vdWE) is employed to grow single crystalline CdS films on mica in order to minimize the

influence of the substrate, since vdWE is known to have less impact on overlayers as compared to chemical epitaxy.²⁴ Recently, vdWE has attracted great interest, thanks to its ability to accommodate large mismatched film-substrate systems. Significant contributions have been made to better understand this field.^{25,26} But note that the absence of interface chemical bonding in vdWE does not necessarily mean the absence of any interface interaction. In fact, strain could even be produced at the heterojunctions of the two weakest layered materials in graphene and boron nitride.²⁷ Therefore, although it is weak, we cannot expect zero interface interaction in this CdS-mica system. However, we do expect it to be weak and not to qualitatively impact our study of the temperature effect. For the temperature effect, we propose an explanation resting on the known entropy difference of hexagonal close-packed (HCP) and face-centered cubic (FCC) atom configurations, corresponding, respectively, to W and ZB here. Then, we take the substrate symmetry into account and explain the discrepancies in reported effects of the substrate temperature and crystal structure.

Table I lists the deposition parameters of CdS films. Experimental details can be found in the supplementary material. W and ZB CdS are essentially the same in the crystal structure except the stacking sequence of the close-packed planes, that is, ABABAB in W and ABCABC in ZB. Since this difference should not affect the spacing between close-packed planes, supposedly, W and ZB CdS share plenty of Bragg peak positions in a XRD $\theta/2\theta$ scan. In this

²Department of Materials Science and Engineering, Rensselaer Polytechnic Institute, Troy, New York 12180, USA

a) Author to whom correspondence should be addressed. Electronic mail: sunx12@rpi.edu

TABLE I. Deposition parameters and XRD microstructural properties of CdS thin films.

	Deposition parameters			XRD microstructural properties				
Sample	Substrate temperature (°C)	Deposition rate (Å/s) ^a	Thickness (nm) ^a	Phase	FWHM of W(0002) or ZB(111) rocking curve (°)	FWHM of W{1011} and/or ZB{111} azimuthal scan (°)		
Film 1	No Intentional Heating (40–90)	0.5	200	W	1.93	8.56		
Film 2	No Intentional Heating (40–90)	6	200	W	4.94	16.15		
Film 3	No Intentional Heating (40–90)	2	200	W	1.87	13.81		
Film 4	140	2	200	W+ZB	1.84	W-8.40; ZB-9.26		
Film 5	300	2	200	/	/	/		
Film 6	300	2	650	ZB	1.38	9.72		

^aThe deposition rate and thickness are based on the reading of a built-in quartz crystal microbalance (QCM). These parameters serve the purpose of reference and may deviate from the actual values. Especially, the deviation may be relatively large for heated substrates since the QCM is water-cooled during depositions and the sticking coefficient of CdS is known to be temperature dependent. In other words, Films 4–6 may be somewhat thinner than indicated.

work, two CdS peaks at 2θ of 26.4° and 54.4° are identified for each of the Films 1–4 and Film 6 (Fig. S1, supplementary material). Note that Film 5 is replaced with Film 6 for XRD since the former is too thin to characterize. We believe that this problem is caused by the low sticking coefficient of CdS at a high substrate temperature. ²⁸ The peaks in the $\theta/2\theta$ scan could be attributed to W (0002)/ZB (111) and W (0004)/ZB (222) reflections. To find out the phase and texture of these films, X-ray pole figure analysis is performed. To this end, 2θ is set at 28.4° to collect the {1011} poles of the W phase at the polar chi angle χ of $\sim 62^{\circ}$. As shown in Figs. 1(a)-1(d), Films 1–4 all present six-fold symmetrical $\{10\overline{1}1\}$ poles at the expected γ positions, which means that these films at least contain, if not completely made of, W CdS. Moreover, the pole figures show six separate poles, suggesting the single crystallinity of the films. The inner four poles are attributed to the mica {115} planes, with which, the epitaxial relationship between W CdS and mica can be deduced as follows (also in Fig. 1(e)): mica(001) || CdS W(0001), mica [100] || CdS W [2110], and mica [010] || CdS W [0110].

Since Film 6, deposited at the substrate temperature of $300\,^{\circ}\text{C}$, shows no W $\{10\bar{1}\,1\}$ poles, along with the fact that it has ZB (111) and (222) peaks in the $\theta/2\theta$ scan, it can be concluded that Film 6 is in ZB modification. To verify, the second pole figure analysis is run at 2θ of 26.4° to collect the three-fold ZB $\{111\}$ poles at a different χ of $\sim70^{\circ}$. It turns out that none of the pole figures for Films 1–3, all deposited

without intentional substrate heating, shows the expected ZB {111} poles. Thus, these films can be concluded to be pure W CdS. In contrast, pole figures of Film 4 (Fig. 1(f)) and Film 6 (Fig. 1(g)) exhibit the expected ZB {111} poles, indicating the presence of ZB CdS. Hence, it can be inferred that Film 4 is a mixed W-ZB and Film 6 is a pure ZB. Here, an unexpected observation is the six-fold symmetry of ZB {111} poles as opposed to the expected three-fold. This can be explained by the formation of the ZB {111} rotational twin structure. ¹⁶ Six poles from mica have also been labeled in Fig. 1(f). The epitaxial relationship between ZB CdS and mica can be concluded as follows (also in Fig. 1(h)): mica(001) || CdS ZB(111), mica [100] || CdS ZB [011], and mica [010] || CdS ZB [211].

XRD results suggest that the deposition rate has little effect on the crystal modification of CdS, though it plays a certain role in affecting the crystal quality. See Table I and supplementary material for XRD rocking curves, azimuthal (φ) scans, and SEM images in Figs. S2, S3, and S4, respectively. In contrast, substrate temperature seems to be more important for the crystal modification of the epitaxial CdS films. As per our results, W and ZB phases are favored at low and high ends of substrate temperature, respectively. Mixed phases can be found in between, indicating the change of the favored phase at a transition temperature T_t . With the thermodynamics deduction shown in the supplementary material, it is concluded that $S_w < S_{ZB}$ at T_t , where S_t represents the entropy. Note that the difference between W

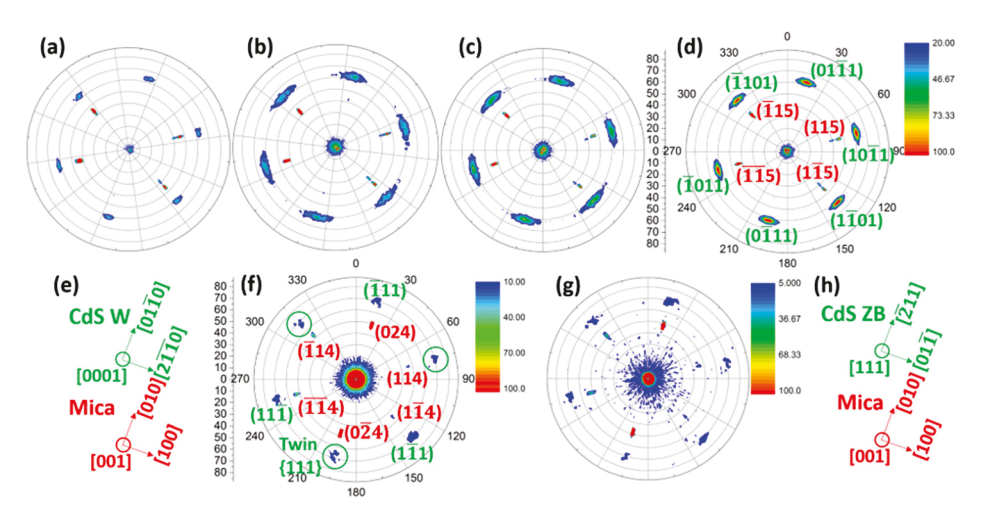


FIG. 1. X-ray pole figures of the epitaxial CdS thin films on mica(001) substrates. (a)-(d) W CdS {1011} pole figures for Films 1–4. The same color scale for all is shown in (d). (e) Epitaxial relationship of Wurtzite CdS(0001) and mica(001) deduced from the pole figures in (a)–(d). (f) and (g) ZB CdS {111} pole figure for Films 4 and 6. (h) Epitaxial relationship of Zinc-blende CdS(111) and mica(001) deduced from the pole figures in (f) and (g).

and ZB structures is analogous to that between HCP and FCC. The hard sphere model has predicted that the entropy difference between FCC and HCP is bounded in [-0.001R] and 0.005R] per mole for all temperatures up to the melting point, where R is the universal gas constant. ^{29–32} While debating on the specific number, it is generally accepted that $S_{FCC} > S_{HCP}$. ³³ Applying to our case of CdS, this model supports our inference that $S_w < S_{ZB}$. Thus, we conclude that this entropy difference between W and ZB CdS is fundamentally responsible for the substrate temperature effect. Note, this discussion involving entropy calculation is qualitative in nature and thus does not come up with a quantitative T_t .

The above analysis is based upon an insignificant influence coming from the substrate crystal structure. This group of CdS-substrate systems can be subdivided into two kinds. The first is the vdWE, where there are no dangling bonds on the surface of substrates for CdS to pair with and all the locking force between CdS and substrates is van der Waals force, which is weak. The second kind is certain chemical epitaxy systems where the lattice mismatch between CdS and substrates is large; thus, the energy benefit from the interface is limited. For these systems, it can be seen from the top portion of Table II that the substrate temperature effect reported in the literature is consistent with our analysis drawn from the entropy difference. Even on non-hexagonal planes of cubic crystals, for example, NaCl(100), 13,15 CdS follows the temperature effect and ignores the substrate crystal structure. In a certain sense, the temperature effect on the crystal modification of CdS can be regarded as an intrinsic property. On the other hand, when a strong extrinsic disturbance, for instance, a highly matching substrate crystal structure, is introduced for CdS epitaxy, the entropy model becomes invalid. The bottom portion of Table II, about 3% or less lattice mismatch, shows that the crystal modification does not correlate with the substrate temperature any more. There are two scenarios for these systems. First, the crystal modification of CdS follows exactly the substrate symmetry when deposited on non-hexagonal planes of cubic crystals. Second, W CdS is more prevailing on hexagonal planes, including the (111) of cubic crystals. Although one report of homoepitaxy indicates a mixed W-ZB, 16 we speculate that kinetics may play a role in that special case. Furthermore, comparing the two portions of Table II, it is noted that the lattice mismatch around 3% is the borderline separating temperature-dominating and interfacedominating regimes. Finally, we propose a more complete explanation regarding temperature and interface effects towards epitaxial CdS films as follows. Intrinsically, CdS tends to be in W modification at low substrate temperature and ZB at high due to the entropy difference between these two structures. Extrinsically, the substrate crystal structure or interface also contributes. For large mismatched systems, the superlattice is formed, and few film lattice points coincide with substrate lattice points, resulting in low density of bonding at the interface.³⁴ Thus, the energy benefit from the interface is not strong enough to outweigh the substrate temperature effect. For small mismatched systems, however, all film lattice points coincide with substrate lattice points, leading to much higher density of bonding at the interface. This energy benefit then becomes too significant to be overcome by the substrate temperature effect.

Figure 2(a) shows the Raman spectra of Films 1-6, along with a reference scan from a bare mica substrate. All films are sufficiently thin such that some or all the peaks from the mica substrate can be observed. For CdS, the longitudinal optical (LO) A₁ phonon mode and its 2nd order overtone (2LO) can be resolved in all films. The magnified view around the 1LO region is shown in Fig. 2(b). Regardless of film deposition parameters, the peak at 264 cm⁻¹ from mica is firmly locked, which serves as a perfect reference to investigate the microstructural change among CdS films. For Films 1-3, the Raman shifts of 1LO are located at 299, 302, and 298 cm⁻¹, respectively, all lower than the counterpart $(\omega_0 = 305 \,\mathrm{cm}^{-1})$ from the bulk CdS. The red-shift compared to the bulk value suggests that Films 1–3 are tensile strained. This can be quantified to be -0.58%, -0.3%, and -0.68%, respectively, using Eq. $(1)^{35}$

$$\frac{\Delta\omega}{\omega_0} = \left(1 + \frac{3\Delta c}{c}\right)^{-\gamma} - 1,\tag{1}$$

where $\Delta\omega$ is the strain-induced shift in the Raman shift between the film and bulk, γ is the Grueneisen parameter (1.1 for CdS), 36 and $\Delta c/c$ is the lattice distortion along the c axis. 35,37 In Refs. 35 and 37, strain-induced shift is defined as the difference between the observed shift and phonon localization-induced shift, which is inversely proportional to the size of nanocrystals. Here, we neglect the latter because our CdS films consist of sufficiently large grains (\sim 60 nm estimated by the Scherrer equation). Among Films 1-3, Film 2 is less strained, which may be explained by its high deposition rate leaving insufficient time for adatoms to fully accommodate, leading to the film structure closer to that of the intrinsic bulk. For Films 3-5, the Raman shifts of 1LO increase from 298 to 300 and 302 cm⁻¹. Note that this blue shift cannot be solely attributed to strain behaviors since it is accompanied by a phase change from W to ZB. Although some experiments have shown that W and ZB CdS have the same 1LO frequency, calculations indicate that the frequency for ZB should be higher.³⁸ If so, then the observed blue shift of the 1LO in Films 3-5 indeed correlates the occurrence of phase change. Furthermore, there is no notable difference in 1LO between Films 5 and 6, suggesting that the thickness has limited effect on the strain in these films.

PL spectra of Films 1-6 are presented in Fig. 2(c). In terms of electron volt, the peak position of the primary PL emissions (2.49, 2.52, 2.46, 2.47, 2.47, and 2.48 eV) trends the similar way as it does in Raman. This indicates that the PL shift likely follows the classical deformation potential theory for CdS, ³⁹ under which, the PL change in these films can be attributed to the varying level of strain and the phase change from W to ZB. PL also suggests that ZB CdS has a larger bandgap than W. In addition, a weak secondary PL emission can be found at the right shoulders of the primary ones for Films 2, 3, 4, and 6 (2.29, 2.33, 2.33, and 2.34 eV). Since this emission is observed in both W and ZB films, it can be excluded from being related to the phase change in CdS. This shoulder peak, largely unknown, may be associated with the photon recycling effect in high quantum efficiency materials.40

TABLE II. Summary of typical epitaxial CdS-substrate systems reported in the literature.

Lattice mismatch ^a (%)	Substrate	Epi plane and direction	CdS phase	Substrate temperature (°C)	Deposition	Characterization	References
30.2	Ag(111)	$Ag(111) CdS(0001), Ag[01\bar{1}] CdS[11\bar{2}0]$	W	170	Evaporation	RHEED ^b	14 and 15
29.9	Ag(111)	$Ag(111) CdS(111), Ag[01\bar{1}] CdS[01\bar{1}]$	W+ZB	400	Evaporation	RHEED	14 and 15
26.4	Mica(0001) ^c	Mica(0001) CdS(111), Mica [10 1 0] CdS [11 2]	ZB	320	Evaporation	RHEED	14
25.7	Mica(0001)	Mica(0001) CdS(0001), Mica [10 \(\bar{1}\) 0] CdS [10 \(\bar{1}\) 0]	W	23	Evaporation	RHEED	14 and 15
23.6	MoS ₂ (0001)	$MoS_2(0001) CdS(0001), MoS_2[11\bar{2}\ 0] CdS[11\bar{2}\ 0] $	W	23	Evaporation	RHEED & TEM ^d	13
23.2	MoS ₂ (0001)	$MoS_2(0001) CdS(111), MoS_2[11\bar{2}\ 0] CdS[1\bar{1}\ 0] $	W+ZB	100-500	Evaporation	RHEED & TEM	13
11.4	InSb(100)	InSb(100) CdS(100)	ZB	350-375	Evaporation	RHEED	16
11.4	InSb(110)	InSb(110) CdS(110)	ZB	350-375	Evaporation	RHEED	16
11.4	InSb(111)	InSb(111) CdS(111)	ZB	350-375	Evaporation	RHEED	16
11.4	CdTe(110)	CdTe(110) CdS(110)	ZB	250	MBE^{e}	RHEED & ARPESf	18
6.6	CaF ₂ (111)	$CaF_2(111) CdS(0001), CaF_2[1\bar{1}0] CdS[11\bar{2}0] $	W	100	Evaporation	RHEED & TEM	13
6.2	CaF ₂ (111)	$CaF_2(111) CdS(111), CaF_2[1\bar{1}\ 0] CdS[1\bar{1}\ 0]$	W+ZB	200-500	Evaporation	RHEED & TEM	13
3.6	NaCl(100)	NaCl(100) CdS(0001), NaCl [110] CdS [11 \(\bar{2}\) 0]	W	23	Evaporation	RHEED	14 and 15
3	NaCl(100)	NaCl(100) CdS(100), NaCl [110] CdS [110]	ZB	280-400	Evaporation	RHEED	14 and 15
Separation	row						
3.3	GaAs(111)	GaAs(111) CdS(001),GaAs [1 $\bar{1}$ 0] CdS [11 $\bar{2}$ 0]	W	200-350; 450	$MOCVD^g$	RHEED & TEM	20, 22, and 23
2.8	GaAs(001)	GaAs(001) CdS(001), GaAs [110] CdS [110]	ZB	200-350; 450	MOCVD	RHEED & TEM	20, 22, and 23
2.5	ZnSe(100)	ZnSe(100) CdS(100)	ZB	27	ALE^h	LEED ⁱ	21
1.2	SrF ₂ (111)	$SrF_2(111) CdS(0001), SrF_2[10\bar{1}][CdS[11\bar{2}0]]$	W	660	CTR^{j}	ED & Ion Blocking	17
0.9	InP(110)	InP(110) CdS(110)	ZB	145-225	MBE	LEED & AES ^k	19
0	CdS(0001)	Homoepitaxy	W	660	CTR	ED & Ion Blocking	17
0	CdS(0001)	Homoepitaxy	W+ZB	300	Evaporation	RHEED	16

^aLattice mismatch is defined as $(a_s-a_f)/a_f$;

^kAuger electron spectroscopy.

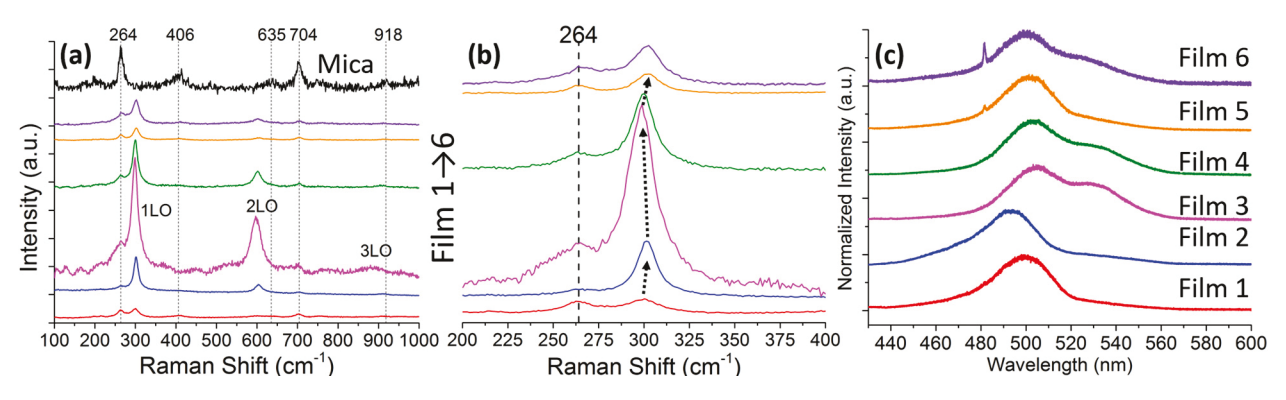


FIG. 2. (a) Raman spectra of Films 1–6 and the bare mica substrate. (b) Magnified view of the CdS 1LO region. The arrows indicate the peak shift among films. (c) Photoluminescence spectra of Films 1–6. The small peaks at \sim 482 nm in Films 5 and 6 are mica's Raman peak. This again suggests these two films to be thinner than others.

In summary, microstructures of vdWE CdS thin films are investigated by decoupling the interface effect. While the deposition rate affects the crystalline quality and strain level in films, it is the substrate temperature that plays a more important role as it directly determines the crystal modification of CdS. The entropy difference model ($S_W < S_{ZB}$) is utilized to explain the temperature effect. On the other hand, for

highly lattice-matched CdS-substrate systems, we find that the interface effect edges over the entropy difference. Raman and PL spectroscopies are used to correlate the microstructural change of films with the observed Raman/PL peak shift.

See supplementary material for details of experimental section, full XRD results, including $\theta/2\theta$ scan, rocking

^bReflection high energy electron diffraction;

[°]Mica is monoclinic (a = 5.199 Å, b = 9.027 Å, c = 20.106 Å, $\alpha = \gamma = 90^{\circ}$, and $\beta = 95.78^{\circ}$), but sometimes mica's $\vec{a} \times \vec{b}$ plane is treated as pseudo-hexagonal, because $2|\vec{a}| \approx |\vec{a} + \vec{b}|$;

^dTransmission electron microscopy;

^eMolecular beam epitaxy;

^fAngle-resolved photoemission spectroscopy;

^gMetalorganic vapor deposition;

^hAtomic layer epitaxy;

ⁱLow energy electron diffraction;

^jChemical transport reaction;

curves, and azimuthal (ϕ) scans, and scanning electron microscopy (SEM) images.

This work was supported by the NYSTAR Focus Center at RPI, C130117 and by NSF Awards under CMMI 1550941, CMMI 1635520, and DMR 1305293. Dr. Zonghuan Lu from Department of Physics, Applied Physics, and Astronomy at Rensselaer Polytechnic Institute is acknowledged for his help on SEM.

- ¹S. G. Kumar and K. S. R. K. Rao, Energy Environ. Sci. **7**(1), 45 (2014).
- ²O. Hayden, A. B. Greytak, and D. C. Bell, Adv. Mater. **17**(6), 701 (2005).
- ³K. Heo, H. Lee, Y. Park, J. Park, H.-J. Lim, D. Yoon, C. Lee, M. Kim, H. Cheong, J. Park, J. Jian, and S. Hong, J. Mater. Chem. **22**(5), 2173 (2012).
- ⁴R. Agarwal, C. J. Barrelet, and C. M. Lieber, Nano Lett. **5**(5), 917 (2005).
- ⁵J. Zhang, D. Li, R. Chen, and Q. Xiong, Nature **493**(7433), 504 (2013).
- ⁶J. Xiao, B. Wen, R. Melnik, Y. Kawazoe, and X. Zhang, Phys. Chem. Chem. Phys. **16**(28), 14899 (2014).
- ⁷C.-Y. Yeh, Z. W. Lu, S. Froyen, and A. Zunger, Phys. Rev. B **46**(16), 10086 (1992).
- ⁸S. Celebi, A. K. Erdamar, A. Sennaroglu, A. Kurt, and H. Y. Acar, J. Phys. Chem. B **111**(44), 12668 (2007).
- ⁹R. Y. Sweeney, C. Mao, X. Gao, J. L. Burt, A. M. Belcher, G. Georgiou, and B. L. Iverson, Chem. Biol. 11(11), 1553 (2004).
- ¹⁰B.-S. Moon, J.-H. Lee, and H. Jung, Thin Solid Films **511–512**, 299 (2006)
- ¹¹O. Zelaya-Angel, F. d. L. Castillo-Alvarado, J. Avendaño-López, A. Escamilla-Esquivel, G. Contreras-Puente, R. Lozada-Morales, and G. Torres-Delgado, Solid State Commun. 104(3), 161 (1997).
- ¹²D. Lincot, B. Mokili, M. Froment, R. Cortès, M. C. Bernard, C. Witz, and J. Lafait, J. Phys. Chem. B **101**(12), 2174 (1997).
- ¹³G. Shimaoka, Thin Solid Films **7**(6), 405 (1971).
- ¹⁴S. Simov, Thin Solid Films **15**(1), 79 (1973).
- ¹⁵K. L. Chopra and I. H. Khan, Surf. Sci. **6**(1), 33 (1967).
- ¹⁶H. Holloway and E. Wilkes, J. Appl. Phys. **39**(12), 5807 (1968).
- ¹⁷W. H. Strehlow, J. Appl. Phys. **41**(4), 1810 (1970).
- ¹⁸D. W. Niles and H. Höchst, Phys. Rev. B 41(18), 12710 (1990).
- ¹⁹W. G. Wilke, R. Seedorf, and K. Horn, J. Vac. Sci. Technol., B 7(4), 807 (1989).

- ²⁰T. Tadokoro, S.-i. Ohta, T. Ishiguro, Y. Ichinose, S. Kobayashi, and N. Yamamoto, J. Cryst. Growth 130(1), 29 (1993).
- ²¹Y. Luo, M. Han, D. A. Slater, and R. M. Osgood, J. Vac. Sci. Technol., A 18(2), 438 (2000).
- ²²A. G. Cullis, P. W. Smith, P. J. Parbrook, B. Cockayne, P. J. Wright, and G. M. Williams, Appl. Phys. Lett. 55(20), 2081 (1989).
- ²³E. Yasuyuki, K. Yoichi, T. Tsunemasa, and H. Akio, Jpn. J. Appl. Phys., Part 2 27(11A), L2199 (1988).
- ²⁴A. Koma, Thin Solid Films **216**(1), 72 (1992).
- ²⁵M. I. Bakti Utama, Q. Zhang, J. Zhang, Y. Yuan, F. J. Belarre, J. Arbiol, and Q. Xiong, Nanoscale 5(9), 3570 (2013).
- ²⁶Y. J. Hong, W. H. Lee, Y. Wu, R. S. Ruoff, and T. Fukui, Nano Lett. 12(3), 1431 (2012).
- ²⁷C. R. Woods, L. Britnell, A. Eckmann, R. S. Ma, J. C. Lu, H. M. Guo, X. Lin, G. L. Yu, Y. Cao, R. V. Gorbachev, A. V. Kretinin, J. Park, L. A. Ponomarenko, M. I. Katsnelson, Y. N. Gornostyrev, K. Watanabe, T. Taniguchi, C. Casiraghi, H. J. Gao, A. K. Geim, and K. S. Novoselov, Nat Phys. 10(6), 451 (2014).
- ²⁸T. Löher, Y. Tomm, C. Pettenkofer, and W. Jaegermann, Appl. Phys. Lett. **65**(5), 555 (1994).
- ²⁹L. V. Woodcock, Nature **385**(6612), 141 (1997).
- ³⁰B. J. Alder, B. P. Carter, and D. A. Young, Phys. Rev. **183**(3), 831 (1969).
- ³¹H. Koch, C. Radin, and L. Sadun, Phys. Rev. E **72**(1), 016708 (2005).
- ³²D. Frenkel and A. J. C. Ladd, J. Chem. Phys. **81**(7), 3188 (1984).
- ³³P. G. Bolhuis, D. Frenkel, S.-C. Mau, and D. A. Huse, Nature 388(6639), 235 (1997).
- ³⁴W. Xie, M. Lucking, L. Chen, I. Bhat, G.-C. Wang, T.-M. Lu, and S. Zhang, Cryst. Growth Des. 16(4), 2328 (2016).
- ³⁵G. Scamarcio, M. Lugará, and D. Manno, Phys. Rev. B 45(23), 13792 (1992).
- ³⁶S. S. Mitra, O. Brafman, W. B. Daniels, and R. K. Crawford, Phys. Rev. 186(3), 942 (1969).
- ³⁷J.-Y. Zhang, X.-Y. Wang, M. Xiao, L. Qu, and X. Peng, Appl. Phys. Lett. 81(11), 2076 (2002).
- ³⁸M. A. Nusimovici and J. L. Birman, Phys. Rev. **156**(3), 925 (1967).
- ³⁹Y. Wang, L. Seewald, Y.-Y. Sun, P. Keblinski, X. Sun, S. Zhang, T.-M. Lu, J. M. Johnson, J. Hwang, and J. Shi, Adv. Mater. 28(40), 8975 (2016).
- ⁴⁰L. M. Pazos-Outón, M. Szumilo, R. Lamboll, J. M. Richter, M. Crespo-Quesada, M. Abdi-Jalebi, H. J. Beeson, M. Vrućinić, M. Alsari, H. J. Snaith, B. Ehrler, R. H. Friend, and F. Deschler, Science 351(6280), 1430 (2016).